Available online at www.sciencedirect.com
ScienceDirect
Thin Solid Films 516 (2008) 8447–8452
thin solid films
www.elsevier.com/locate/tsf

Aluminium incorporation in $Al_xGa_{1-x}N$/GaN heterostructures: A comparative study by ion beam analysis and X-ray diffraction

A. Redondo-Cubero [a,b], R. Gago [b,*], F. González-Posada [a], U. Kreissig [c], M.-A. di Forte Poisson [d], A.F. Braña [a], E. Muñoz [a]

[a] ISOM and Dpt. de Ingeniería Electrónica, ETSI Telecomunicación, Universidad Politécnica de Madrid, E-28040 Madrid, Spain
[b] Centro de Micro-Análisis de Materiales, Universidad Autónoma de Madrid, E-28049 Madrid, Spain
[c] Institute of Ion Beam Physics and Materials Research, Forschungszentrum Dresden-Rossendorf, PF 51019, D-01314 Dresden, Germany
[d] Thales Research & Technology/TIGER 91461 Marcoussis Cedex, France

Received 18 September 2007; received in revised form 14 March 2008; accepted 9 April 2008
Available online 16 April 2008

Abstract

The Al content in $Al_xGa_{1-x}N$/GaN heterostructures has been determined by X-ray diffraction (XRD) and contrasted with absolute measurements from ion beam analysis (IBA) methods. For this purpose, samples with $0.1<x<0.3$ grown by metal organic chemical vapour deposition on sapphire substrates have been studied. XRD and IBA corroborate the good epitaxial growth of the AlGaN layer, which slightly deteriorates with the incorporation of Al for $x>0.2$. The assessment of Al incorporation by XRD is quite reliable regarding the average value along the sample thickness. However, XRD analysis tends to overestimate the Al fraction at low contents, which is attributed to the presence of strain within the layer. For the highest Al incorporation, IBA detects a certain Al in-depth compositional profile that should be considered for better XRD data analysis.

Keywords: AlGaN; HEMT; RBS; ERDA; XRD

1. Introduction

AlGaN/GaN heterostructures (HS) are key structures to fabricate GaN-based quantum building blocks and to perform band gap engineering. In fact the use of one or multiple HS of the (Al,Ga,In)N system has led to present visible and UV light emitting diodes and laser diodes, to Bragg reflectors, superlattices, high electron mobility transistors (HEMT), UV photodetectors, resonant tunnelling diodes, etc. [1,2]. In the case of GaN HEMT a single AlGaN/GaN HS forms a triangular quantum well that host a high-density two dimensional electron gas (2DEG) at the GaN side, that shows excellent transport properties along the AlGaN/GaN interface [1–3]. In this way, both higher carrier velocities and total electron density have been achieved [3]. The outstanding electrical properties of such simple HS has motivated the development of GaN HEMT as the most promising high-power, high frequency transistors. In other GaN-based optoelectronic and electronic devices the active region is usually composed of multiple quantum wells (MQW), and carrier transport is perpendicular to the AlGaInN/InGaN interface [4,5].

In the case of a basic GaN HEMT, tailoring the electrical properties of the AlGaN/GaN HS depends mainly on the AlGaN barrier thickness, typically in the order of 30 nm, and on its Al content (usually in the 0.2 range) [2,3]. The impact of these variables may also be convoluted with the parallel development of strain within the layer, since the AlGaN layer starts growing pseudomorphic to the GaN substrate and then relaxes after reaching a critical thickness [2]. The critical thickness value decreases with the incorporation of Al in the AlGaN layer [6]. The presence of strain in the AlGaN layer has relevant implications for the 2DEG properties through the polarization fields developed and subsequent effects on the 2DEG [7].

* Corresponding author. Tel.: +34 914973074; fax: +34 914973623.
E-mail address: raul.gago@uam.es (R. Gago).

0040-6090/$ - see front matter © 2008 Elsevier B.V. All rights reserved.
doi:10.1016/j.tsf.2008.04.069

From the above, control and reproducibility of the electrical properties of AlGaN/GaN HS imposes a good control over the layer stoichiometry and growth process. X-ray diffraction (XRD) analysis is frequently used as a routine technique for the determination of the Al incorporation, x, in the $Al_xGa_{1-x}N$ layer [8]. This method provides information about the Al content indirectly, since it is deduced from the relative shift of the $Al_xGa_{1-x}N$ reflection with respect to the GaN one. However, as it is well known, the shift in the peak can also be influenced by the presence of strain within the layer, making the analysis ambiguous [9]. Another disadvantage of the XRD analysis is that an Al profile analysis is not straightforward and may require tedious techniques, such as changing the incidence angle to explore different layer depths.

Although high resolution XRD is quite well established in the epitaxial growth community as the tool to determine Al fraction in AlGaN/GaN HS, the motivation of the present work is to conduct a comparative study about the determination of the Al content by comparing XRD results with other methods providing univocal and absolute values of composition. In this context, ion beam analysis (IBA) techniques are one of the most powerful techniques to assess compositional depth profiles in thin films and coatings [10]. Another advantage of IBA methods is their non destructive character. The suitability of these techniques to study GaN-based materials has been already reported [11]. Among IBA methods, Rutherford backscattering spectrometry (RBS) has been used to contrast with XRD analysis in AlGaN layers [9] and superlattices [12]. The advantage of RBS is that it can provide additional structural information by performing RBS in channelling mode (RBS/C) [13,14]. However, Al determination by RBS is not easy when heavier elements are present in the matrix, such as Ga, due to signal overlapping. This drawback can be overcome with non-Rutherford or nuclear reaction analysis [15], although the analysis become more complex and a precise knowledge of the scattering cross-section is needed. Heavy-ion elastic recoil detection analysis (HI-ERD) with time-of-flight or ionisation chamber detectors presents mass or Z-resolved signals, respectively, and can alternatively be used to increase the Al sensitivity due to the lack of signal overlap [12].

Although RBS has been already applied to study the Al content in AlGaN structures, a systematic comparative study of Al incorporation by RBS and XRD has not yet been addressed. Here, we study the evolution of $Al_xGa_{1-x}N$ layers with Al incorporation in the $0.1<x<0.3$ range. The quantification of the Al content by RBS is corroborated by HI-ERD. In addition, the crystalline quality and in-depth homogeneity of the epitaxial layer, as Al incorporation increases, can be contrasted with RBS/C and XRD results. Our results indicate that XRD is quite reliable in the determination of the average Al content within the layer. However, for Al incorporation $x>0.2$, a slight Al composition profile and dechanneling effects are detected. At low Al compositions the presence of strain leads to XRD results tending to overestimate the Al fraction.

2. Experimetal details

$Al_xGa_{1-x}N$/GaN HS with x values ranging from 0.1 to 0.3 were grown by metal organic chemical vapour deposition. Although initial experiments were performed in samples with AlGaN layers in the 30 nm range, difficulties in clear assessment by IBA led us to consider thicker barriers. In all the samples, the HS was grown on sapphire substrates and consists of a 150 nm thick undoped AlGaN top-most layer followed by a 1.2 μm GaN buffer.

High-resolution XRD measurements were taken in a 3D Bede Scientific Diffractometer using the θ–2θ configuration around the symmetric (00.2) and asymmetric (10.5) reflections, the latter under steep and shallow incidence. The symmetric and asymmetric reflections provide information about crystalline planes parallel and perpendicular to the sample surface, respectively. In addition, the width of the reflections scales with the number of dislocations present in the crystal growth [16]. The Al composition and degree of relaxation (R) in the AlGaN layer affect the relative shifts of the symmetric and asymmetric reflections with respect to the reference GaN substrate. The values are extracted by fitting the experimental scans with a dynamical XRD model [17].

RBS experiments were performed at the 5 MV Cockroft–Walton tandetron accelerator of Centro de Micro-Análisis de Materiales at UAM (Madrid, Spain). The measurements were carried out with 2 MeV $^4He^+$ beam and the backscattered ions were detected with a silicon implanted barrier detector (energy resolution of 15 keV) located at scattering angle of 170 in the IBM geometry. Random and channelling (RBS/C) spectra along the [0001] crystallographic orientation were taken in the same run. Random RBS and RBS/C spectra were simulated by the RBX code [18].

HI-ERD was acquired with a Bragg ionisation chamber (BIC) at the Center for "Applications of Ion Beams in Materials Research" (AIM) of Forschungszentrum Dresden-Rossendorf (FZD) (Dresden, Germany). The ERD-BIC experiments were performed with 40 MeV Cl^{8+} at a grazing incidence angle of 10 and at a scattering angle of 30°. Additionally, a Si detector was placed at a scattering angle of 38° for H detection. The detector was covered with an Al-range foil to suppress all scattered ions and recoils apart from H.

3. Results and discussion

3.1. X-ray diffraction analysis

Fig. 1 shows the high resolution XRD scans from (00.2) and (10.5) reflections. It can be appreciated that the AlGaN reflection shifts to higher angles, in correlation with an increase in the Al content (change in the lattice parameter). The Al content and degree of relaxation has been extracted from fitting the symmetric and asymmetric (under steep and shallow incidence) reflections simultaneously. The samples were under strain ($R<0.05$) except for the one with the highest Al content. In this case, the sample was partially relaxed ($0<R<0.2$). This change is not surprising since the critical thickness for strain relaxation

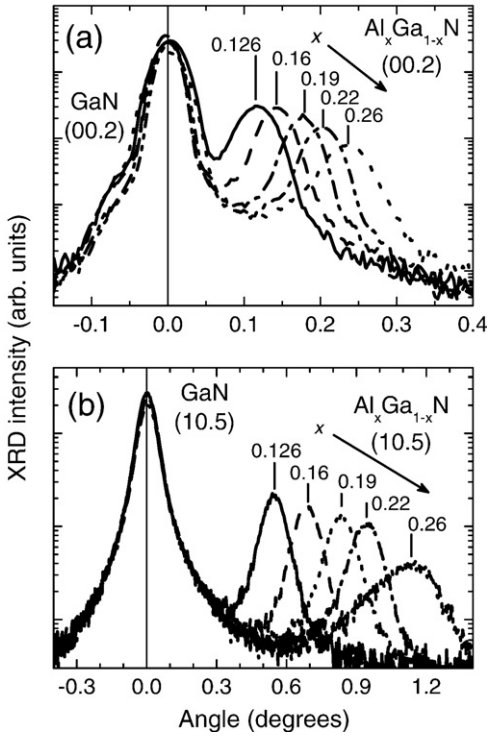

Fig. 1. Experimental high resolution XRD scans in the θ/2θ configuration for the symmetrical (00.2) (a) and asymmetrical (10.5) (b) reflections for samples with different Al contents (x). The peak position for the AlGaN reflection shifts to higher angles with the Al incorporation.

scales with the Al incorporation and falls in the range of ~100 nm for the Al contents used in this work [6].

The full width at half maximum (FWHM) of the XRD reflections reveals the good crystalline and epitaxial quality of the layers. The evolution of the FWHM upon Al incorporation in the AlGaN layer is displayed in Fig. 2. The FWHM of the (00.2) reflection remains nearly constant and starts to increase for $x>0.2$. A sharp increase is also found in the FWHM of the (10.5) reflection under shallow incidence, where the configuration is more sensitive to strain, for the largest Al content ($x\sim26$). The previous trends indicate that the sample crystallinity slightly deteriorates upon Al incorporation above $x\sim0.2$ and that the strain within the layer is relevant for the largest Al content.

3.2. Ion beam analysis

Fig. 3 shows the random and aligned RBS spectrum of an $Al_xGa_{1-x}N$/GaN sample with $x\sim0.26$, as derived from the XRD data. The contribution from the different elements to the spectrum is highlighted in the graph with labels. For each element, the energy range correlates with a depth scale (closer to the surface the higher the energy). Due to the heavy mass of Ga, the RBS detection of this element presents a high cross-section. This high sensitivity for Ga and the signal overlap is detrimental in this case, since imposes a reduced sensitivity to Al and N detection. The Ga signal presents a step in the surface region (higher energy channels) due to the Ga deficiency in the AlGaN layer. Hence, the increase in the Al incorporation in the films reflects in a decrease in the Ga signal in this region. In this case, the Al content can be determined by the deficiency in Ga and assuming that a stoichiometric nitride, i.e. N content of 50 at.%. This analysis implies an error of 10% in the calculation of x.

The simulation of the random RBS spectra was performed with a simple two-layer model to describe the AlGaN/GaN HS. This worked out successfully except for the sample with $x=0.26$, where to fit results the AlGaN layer had to be divided into two regions (contributions) for a proper simulation of the experimental spectrum (see Fig. 3). In particular, an $Al_{0.22}Ga_{0.78}N$ layer (~30 nm) closer to the AlGaN/GaN interface and an Al-richer layer ($Al_{0.28}Ga_{0.72}N$) near surface are deduced. This indicates a gradient in the Al concentration, with an average composition closer to the value extracted from XRD ($x\sim0.26$). The presence of an Al profile could be related to the AlN limited solubility in the GaN matrix [19]. The Al profile should be taken into account when modelling the HEMT electrical properties since it implies a lower Al concentration closer to the 2DEG region.

Epitaxial growth of the ternary layer was assessed from aligned [0001] spectra, since minimum yield (χ_{min}) is the main parameter determining crystalline quality with depth resolution [13]. Low values of χ_{min} (2–5%) correspond to layers with a good crystalline quality, while high values evidence defects on the growth. RBS/C analysis of the $Al_{0.26}Ga_{0.74}N$/GaN HS (lower graph and inset in Fig. 3) reveals a minimum yield $\chi_{min}=2.4\%$ (for the Ga signal close to the surface), but it can be as good as 1.7% for samples with $x<0.16$. These values

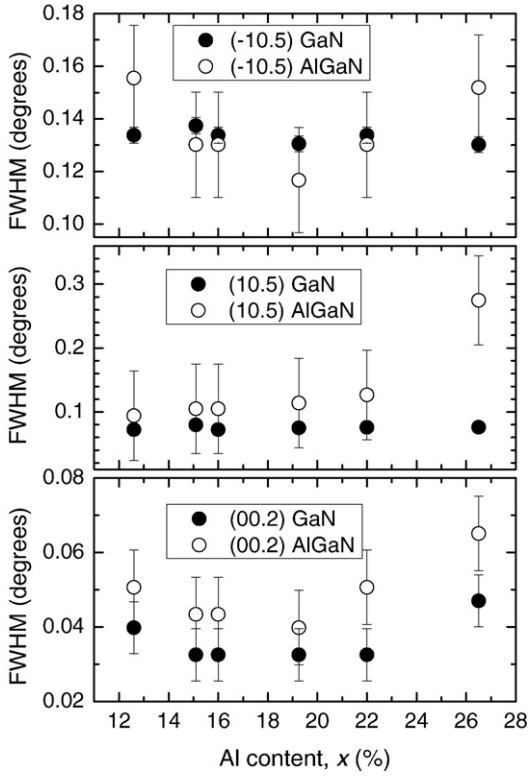

Fig. 2. FWHM for (00.2) and (10.5) reflections of the GaN and AlGaN phases.

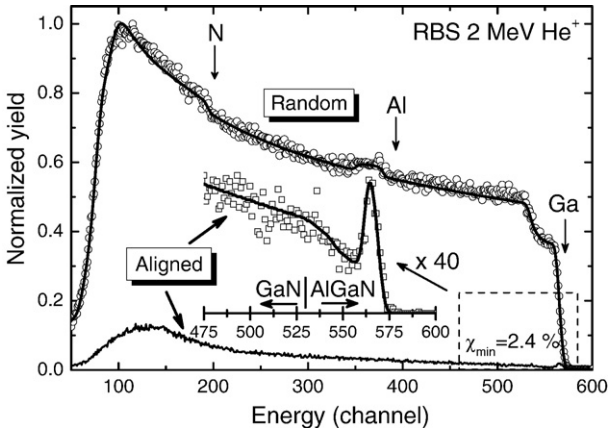

Fig. 3. Random and [0001] aligned RBS spectra of an $Al_{0.26}Ga_{0.74}N$/GaN HS, together with the simulation curves (solid lines). The decrease in the crystalline quality of the AlGaN/GaN HS is shown by the increase in dechanneling at the HS interface (inset).

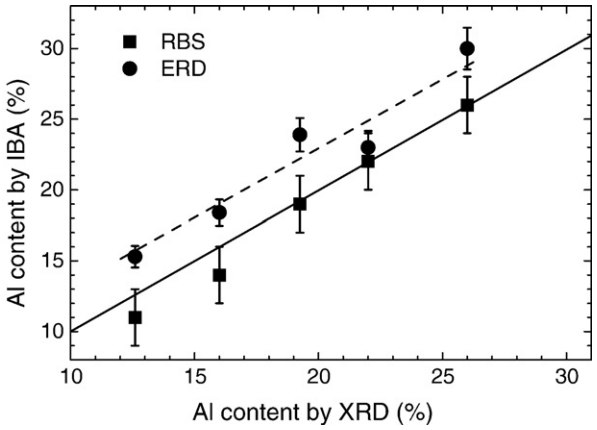

Fig. 5. Comparison of the Al content determined by XRD and ion beam analysis methods. RBS agrees with XRD except for low Al concentration samples. Mean values were taken for IBA when spectra showed depth concentration profiles.

confirm the excellent epitaxial growth of the AlGaN alloy, also verified by XRD measurements. Indeed, the χ_{min} values obtained for the AlGaN layer are comparable to commercial GaN templates and as good as best values shown in literature [20,21]. However, a significant increasing of dechanneling can be observed when Al incorporation is high ($x>0.2$). In particular, sample with $x\sim0.26$ revealed a higher dechanneling in the $Al_xGa_{1-x}N$ layer in comparison to the GaN buffer layer (note the slope change in the signal yield for the enlarged RBS/C spectrum in the inset of Fig. 3). This fact may be related with the observed profile in the random spectra. Indeed, following Vegard's law [22], these profiles indicate that a different lattice parameter is present for the grown AlGaN structure, explaining the rising of dechanneling. These observations regarding the sample dechanneling are consistent with the XRD trends displayed in Fig. 2.

Some information regarding the GaN/Al_2O_3 interface can be obtained from the RBS Ga signal (energy channels from 50 to 100 in Fig. 3). Here, a clear increase of dechanneling appears since the RBS/C yield reaches ~12% of the random value. This fact has been already reported in other GaN based HS [20,23] and can be easily explained by the lattice mismatch between sapphire and GaN (close to 14%).

In order to improve the sensitivity to light elements, such as Al and N, ERD-BIC experiments were performed. The spectrum of an HS with $x=0.126$ (derived from XRD) is shown in Fig. 4(a). As clearly observed, the signal from Al and N are well separated overcoming the limitations of RBS. Since Ga is heavier than the Cl^{8+} projectiles, the probability of getting Ga recoils is rather low and, in addition, the Ga recoil line overlaps with the main contribution of scattered projectiles. Therefore, the Ga contribution

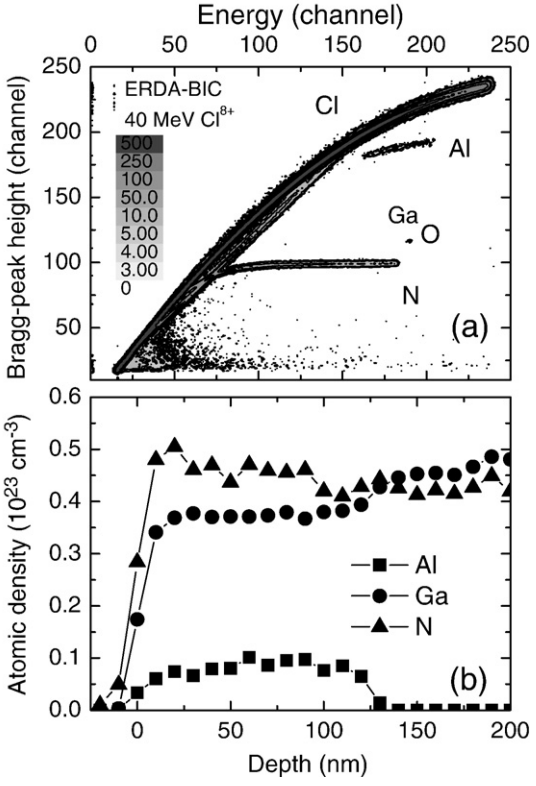

Fig. 4. (a) ERD-BIC spectrum of $Al_{0.14}Ga_{0.86}N$/GaN structure using 40 MeV Cl^{8+} ions. (b) Elemental depth profiles obtained from the analysis of the ERD-BIC spectra. A regular 125 nm depth profile is visible for Al.

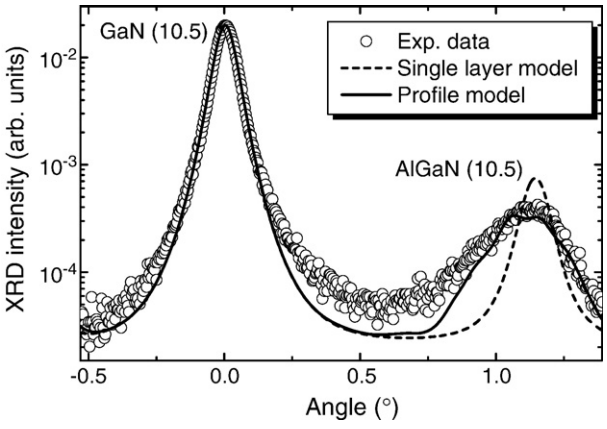

Fig. 6. Correlation between the experimental high resolution XRD data for the (10.5) reflection and simulations considering a single AlGaN layer ($x=0.26$) and the in-depth profile detected by RBS.

can be obtained from the high-energy side of the scattered Cl^{8+} ions, corresponding to scattered projectiles from Ga atoms (i.e. RBS signal). The ERD-BIC spectra also show some slight oxygen contamination of the surface and a negligible amount of H.

Due to the well-separated N, Al and Ga signals, concentration sensitivity is increased to less than 5%. The analysis of the individual elements yields the compositional profile shown in Fig. 4(b), being the average value of the x parameter ($x \sim 0.14$ for the mentioned sample) calculated by integration of the signals. The most important conclusion of this calculation is that the N content in the layer is constant and close to 50%. The achievement of stoichiometric $Al_xGa_{1-x}N$ layers is relevant for the crystalline quality of the layers [3]. In addition, these measurements justify the hypothesis used in the RBS simulations, where the N content was fixed to 50% to attain the Al value.

3.3. Comparison of the different results

Fig. 5 resumes the results obtained from all the analytical methods employed. The main conclusion that can be extracted from the results is the very good agreement between RBS and XRD analysis. Despite this trend, a slight overestimation of the Al content by XRD is attained for small Al incorporation ($x < 0.18$). Although x can be determined by XRD independently of R using the (10.5) reflection under steep X-rays incidence (configuration which is less sensitive to strain), the simulation does not allow to distinguish between $R = 0$ and $R < 0.05$ states. Thus, the residual strain could still affect the estimation of x as derived from the XRD data, explaining the deviation from our RBS results. It should be noted that XRD gives average values whereas RBS has shown the presence of in-depth profiles, specially in the sample with the highest Al content ($x = 0.26$). This fact points out some additional considerations that cannot be directly extracted from the XRD data alone. This ambiguous analysis has also been addressed in other studies. For example, a double peak structure in the XRD scans for InGaN/GaN HS have been related to strained and pseudomorphic components with the same composition and not, as would be presumably assumed, to phase segregation within the layer [24].

The presence of an in-depth Al profile observed from RBS can be used to improve the XRD analysis. This is shown in Fig. 6, where XRD simulations considering a single layer model or an in-depth profile are displayed. In this latter case, the same layer model as derived from the RBS analysis has been assumed, together with a relaxation parameter $R < 0.05$. It is clear that the correlation between the experimental and simulated data is strongly improved by considering the Al profile. Considering the error in the simulation, the effect of strain relaxation cannot be completely ruled out. Nevertheless, simulations show that R is mainly affecting the peak position and only playing a minor role in the peak broadening. Consequently, the fitting of XRD data cannot be achieved based on the single assumption of film relaxation and the incorporation of different Al contents is necessary.

Finally, as shown in Fig. 5, ERD-BIC results reproduce the trend of the Al incorporation in the samples obtained from RBS. However, a systematic deviation from the ERD-BIC values with respect to RBS is observed, with an overestimation in the Al concentration. This fact could be explained by uncertainties in the scattering cross-section and deviations from the Rutherford formula regarding the collision events of Ga ions with light elements. It should be mentioned that the Ga content is derived from the Cl^{8+} scattered ions while the contribution of light elements is extracted from the recoil atoms (N and Al).

4. Conclusions

We have carried out a comparative compositional study by XRD and IBA methods of $Al_xGa_{1-x}N$/GaN HS. Samples with different Al contents, $0.1 < x < 0.3$, have been studied to validate the reliability of indirect analysis by XRD in contrast to absolute values obtained from IBA methods. The limited sensibility of RBS to Al, due to the presence of heavy elements in the atomic matrix such as Ga, has been overcome by complementary ERD-BIC analysis.

It can be concluded that the estimation of the Al content by XRD is quite reliable and in very good agreement with IBA data. Our study shows that the values extracted from XRD data are averaged over the sampling depth of the technique. Also, a slight overestimation of the average content is found when strain is present in the films.

XRD and RBS/C data have shown the good crystalline and epitaxial quality of the layers. However, this quality slightly deteriorates for increasing Al incorporation in the AlGaN layer for $x > 0.2$. In parallel, an in-depth Al profile has been observed for the largest Al content ($x \sim 0.26$). The information given by IBA techniques regarding the presence of compositional profiles represents an important feedback for improvement of XRD characterisation.

Acknowledgements

We are to indebt to Ángel Muñoz-García for his help with the RBS/C acquisition software. This work has been carried out inside the KORRIGAN project (EU-FP6 contract no. MOU 04/102.052/032). The experiments at AIM (FZD-Rossendorf) were supported by the EU-"Research Infrastructures Transnational Access" program under EC contract no. 025646.

References

[1] O. Ambacher, J. Smart, J.R. Shealy, N.G. Weimann, K. Chu, M. Murphy, W.J. Schaff, L.F. Eastman, R. Dimitrov, L. Wittmer, M. Stutzmann, W. Rieger, J. Hilsenbeck, J. Appl. Phys. 85 (1999) 3222.
[2] M. Fieger, M. Eickelkamp, L. Rahimzadeh Koshroo, Y. Dikme, A. Noculak, H. Kalisch, M. Heuken, R.H. Jansen, A. Vescan, J. Cryst. Growth 298 (2007) 843.
[3] G.Y. Zhao, H. Ishikawa, T. Egawa, T. Jimbo, M. Umeno, Physica E 7 (2000) 963.
[4] F.A. Ponce, D.P. Bour, Nature 386 (1997) 351.
[5] M. Umeno, T. Egawa, H. Ishikawa, Mater. Sci. Semicond. Process 4 (2001) 459.
[6] S.R. Lee, D.d Koleske, CrossK.C. , FloroJ.A. , WaldripK.E. , WiseA.T. , MahajanS. , Appl. Phys. Lett. 85 (2004) 6164.
[7] B. Shen, T. Someya, Y. Arakawa, Appl. Phys. Lett. 76 (2000) 2746.

[8] X. Wang, C. Wang, G. Hu, H. Xiao, C. Fang, J. Wang, J. Ran, J. Li, J. Li, Z. Wang, J. Cryst. Growth 298 (2007) 791.
[9] M.F. Wu, S. Yao, A. Vantomme, S.M. How, G. Langouche, J. Li, G.Y. Zhang, J. Vac. Sci. Technol. B 17 (1999) 1502.
[10] J.R. Tesmer, M. Nastasi (Eds.), Handbook of Modern Ion Beam Material Analysis, Materials Research Society, 1995, Pittsburg (USA).
[11] E. Alves, N.P. Barradas, T. Monteiro, R. Correira, U. Kreissig, Nucl. Instrum. Methods Phys. Res., Sect. B 188 (2002) 73.
[12] S. Zhou, M.F. Wu, S.D. Yao, B.S. Zhang, H. Yang, Superlattices Microstruct. 40 (2006) 137.
[13] L.C. Feldman, J.W. Mayer, S.T. Picraux, Materials analysis by ion channelling, Academic Press, London (UK), 1982.
[14] D.S. Gemmell, Rev. Mod. Phys. 46 (1974) 129.
[15] M.J.F. Healy, A.J. Pidduck, G. Dollinger, L. Gorgens, A. Bergmaier, Nucl. Instrum. Methods Phys. Res., Sect. B 190 (2002) 630.
[16] S.D. Hersee, J.C. Ramer, K.J. Malloy, MRS Bull 22/7 (1997).
[17] O. Brandt, P. Waltereit, K.H. Ploog, J. Phys. D 35 (2002) 577.
[18] E. Kótai, Nucl. Instrum. Methods Phys. Res., Sect. B 85 (1994) 588.
[19] S. Krukowski, Diam. Relat. Mater. 6 (1997) 1515.
[20] M.F. Wu, A. Vantomme, S. Hogg, G. Langouche, W. Van der Stricht, K. Jacobs, I. Moerman, Nucl. Instrum. Methods Phys. Res., Sect. B 174 (2001) 181.
[21] J.C. Zhang, M.F. Wu, J.F. Wang, J.P. Liu, Y.T. Wang, J. Chen, R.Q. Jin, H. Yang, J. Cryst. Growth 270 (2004) 289.
[22] L. Vegard, Z. Phys. 5 (1921) 17.
[23] B. Holländer, S. Mantl, M. Mayer, C. Kirchner, A. Pelzmann, M. Kamp, S. Christiansen, M. Albrecht, H.P. Strunk, Nucl. Instrum. Methods Phys. Res., Sect. B 136 (1998) 1248.
[24] S. Pereira, M.R. Correia, E. Pereira, K.P. O, Donnell, E. Alves, A.D. Sequeiro, N. Franco, Appl. Phys. Lett. 79 (2001) 1432.